

# Inventory of Load Models in Electric Power Systems via Parameter Estimation

Kevin Wedeward, Chris Adkins, Steve Schaffer, Michael Smith, and Amit Patel

**Abstract**—This paper presents an approach to characterize power system loads through estimation of contributions from individual load types. In contrast to methods that fit one aggregate model to observed load behavior, this approach estimates the inventory of separate components that compose the total power consumption. Common static and dynamic models are used to represent components of the load, and parameter estimation is used to determine the amount each load contributes to the cumulative consumption. Trajectory sensitivities form the basis of the parameter estimation algorithm and give insight into which parameters are well-conditioned for estimation. Parameters of interest are contributions to total load and initial conditions for dynamic loads. Results are presented for two simulation-based studies and demonstrate the feasibility of the approach. In the first study, the composition of multiple loads connected to a bus was estimated by subjecting the bus to a step change in voltage. The second study utilized a disturbance in the WSCC nine-bus test system to facilitate estimates of the combination of loads connected at a bus in the system.

**Index Terms**—electric power systems, load modeling, simulation, trajectory sensitivities, parameter estimation, measurement-based, load inventory.

## I. INTRODUCTION

As power system models and simulations used for planning and stability studies become more advanced, higher fidelity models of all power system components are needed. Loads are particularly difficult to describe due to their diverse composition and variation in time, yet their importance to dynamic behavior and stability of the overall power system has been recognized [1]–[8]. While a variety of load models have been adopted (for example, see [3], [9]), the approaches to load modeling can typically be categorized as either measurement-based or component-based [8]. Measurement-based approaches utilize data collected from a substation or feeder to develop a model that matches observed behavior [10]–[22]. Disturbances such as a loss of load or power line, or movement of an under load tap changer (ULTC) are often needed to have measurements sufficiently rich for effective measurement-based techniques. Advances in technology such as power quality meters, disturbance monitors and Phasor Measurement Units (PMUs) with the ability to sample at high rates have facilitated growth in measurement-based approaches. Component-based approaches combine a knowledge of the load and known models of all devices that make up the load for simulation, analysis and/or aggregation [5], [8], [23]–[26]. A combination of the approaches, known as identification of load inventory, has been developed where measurements are used to estimate the amount (e.g., fraction

or percentage) each set of similar devices within a load contributes to the aggregate power consumed [18], [27]–[30].

The focus of this paper is development of a load inventory model where parameter estimation is used to determine the amount each component contributes to the total power consumption. Parameter estimation is achieved via a Gauss-Newton method based upon trajectory sensitivities (see [31], [32] for background and other applications) which computes parameters that best fit simulated model responses to simulated measurements on a single phase. The results indicate which load contributions are well-conditioned for estimation and that those parameters can be accurately estimated in the presence of measurement error. Initial conditions of the dynamic states in the load models are difficult to identify; however, the load contribution coefficients are identifiable.

## II. LOAD MODELING

A wide variety of load models exist to mathematically represent the power consumed by a load and its dependencies on voltage, frequency, type and composition. Three common mathematical models for loads in power systems are presented below and utilized in the proposed approach. In all cases, it is assumed that powers and voltages are normalized by base values such that their units are in per unit (p.u.) [33], [34].

### A. ZIP

A polynomial model is commonly used to represent loads and capture their voltage dependency. The average and reactive powers of the load are written as a sum of constant impedance ( $Z$ ), constant current ( $I$ ) and constant power ( $P$ ), and referred to as the ZIP model [4], [34].

$$P = P_0(K_{1p} \left(\frac{V}{V_0}\right)^2 + K_{2p} \frac{V}{V_0} + K_{3p}) \quad (1)$$

$$Q = Q_0(K_{1q} \left(\frac{V}{V_0}\right)^2 + K_{2q} \frac{V}{V_0} + K_{3q}) \quad (2)$$

where  $P$ ,  $Q$  are the average and reactive power consumed by the load, respectively,  $P_0$ ,  $Q_0$  represent the nominal average and reactive power of the load, respectively,  $V$  is the magnitude of the sinusoidal voltage at the bus to which the load is connected,  $V_0$  is the magnitude of the nominal voltage at the bus, and coefficients  $K_{1p}$ ,  $K_{2p}$ ,  $K_{3p}$ ,  $K_{1q}$ ,  $K_{2q}$  and  $K_{3q}$  define the proportion of each component of the model. Coefficients for many load types have been experimentally determined and reported [5], [8], [11], [12], [17].

Manuscript submitted on February 4, 2015.

Kevin Wedeward, Chris Adkins, Steve Schaffer, and Michael Smith are with the Institute for Complex Additive Systems Analysis (ICASA), New Mexico Institute of Mining and Technology, Socorro, NM 87801 USA, email: wedeward@nmt.edu.

Amit Patel is with Accenture, Irving, TX 75039 USA.

### B. Exponential Recovery

The power profile is defined by

$$P = \frac{x_p}{T_p} + P_0 \left( \frac{V}{V_0} \right)^{\alpha_t} \quad (3)$$

$$Q = \frac{x_q}{T_q} + Q_0 \left( \frac{V}{V_0} \right)^{\beta_t} \quad (4)$$

where  $P$ ,  $Q$  are the average and reactive power consumed by the load, respectively,  $P_0$ ,  $Q_0$  are the nominal average and reactive power, respectively,  $V$  is the magnitude of the sinusoidal voltage at the bus to which the load is connected, and  $V_0$  is the magnitude of the nominal voltage at the bus. Parameters  $T_p$  and  $T_q$  are the average and reactive load recovery time constants, respectively,  $\alpha_s$  and  $\beta_s$  are the steady-state dependence of average and reactive powers on voltage, respectively, and  $\alpha_t$  and  $\beta_t$  are the transient dependence of average and reactive powers on voltage, respectively. The parameters govern the behavior of the load model, and are generally fit to measurements. States  $x_p$  and  $x_q$  are average and reactive power recovery, respectively, and are governed by the differential equations [15], [35], [36]:

$$\dot{x}_p = \frac{-x_p}{T_p} + P_0 \left( \left( \frac{V}{V_0} \right)^{\alpha_s} - \left( \frac{V}{V_0} \right)^{\alpha_t} \right) \quad (5)$$

$$\dot{x}_q = \frac{-x_q}{T_q} + Q_0 \left( \left( \frac{V}{V_0} \right)^{\beta_s} - \left( \frac{V}{V_0} \right)^{\beta_t} \right). \quad (6)$$

Parameters for different load types have been experimentally determined and reported [15], [36].

### C. Induction Motor

The induction motor's voltages of interest are  $V e^{j\theta} = V \cos(\theta) + jV \sin(\theta)$  at the stator terminal and  $V' e^{j\theta'} = v'_d + jv'_q$  at the voltage behind transient reactance. The stator current is  $I = i_d + ji_q = \frac{V e^{j\theta} - V' e^{j\theta'}}{R_s + jX'_s}$  where  $X'_s = X_s + \frac{X_r X_m}{X_r + X_m}$  is the transient reactance. Additional parameters are stator resistance and leakage reactance,  $R_s$  and  $X_s$ , respectively, magnetizing reactance,  $X_m$ , and rotor resistance and leakage reactance,  $R_r$ ,  $X_r$ , respectively. The transient equivalent circuit for the induction motor with voltages, currents and parameters labeled is shown in Figure 1.

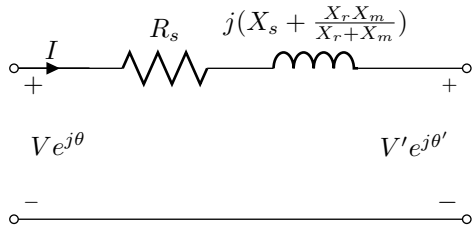


Fig. 1. Transient-equivalent circuit of induction motor

The voltage  $V' e^{j\theta'} = v'_d + jv'_q$  has real and imaginary parts governed by the differential equations [34], [37]

$$\frac{dv'_d}{dt} = -\frac{R_r}{X_r + X_m} \left[ v'_d + \left( \frac{X_m^2}{X_r + X_m} \right) i_q \right] + s v'_q \quad (7)$$

$$\frac{dv'_q}{dt} = -\frac{R_r}{X_r + X_m} \left[ v'_q - \left( \frac{X_m^2}{X_r + X_m} \right) i_d \right] - s v'_d \quad (8)$$

$$\frac{ds}{dt} = \frac{1}{2H} \left( T_{mo} (1-s)^2 - T_e \right) \quad (9)$$

where  $s = \frac{\omega_s - \omega_r}{\omega_s}$  is slip,  $\omega_r$  is rotor speed,  $\omega_s$  is angular velocity of the stator field,  $T_{mo}$  is a load torque constant,  $T_e = v'_d i_d + v'_q i_q$  is electromagnetic torque, and  $H$  is the motor and motor load inertia.

The average power  $P$  and reactive power  $Q$  consumed by the motor are then given by

$$P = \text{Re}(V e^{j\theta} I^*) = \frac{1}{R_s^2 + X_s'^2} \left( R_s (V^2 + V \cos(\theta) v'_d - V \sin(\theta) v'_q) - X_s' (V \cos(\theta) v'_q - V \sin(\theta) v'_d) \right) \quad (10)$$

$$Q = \text{Im}(V e^{j\theta} I^*) = \frac{1}{R_s^2 + X_s'^2} \left( R_s (V \cos(\theta) v'_q - V \sin(\theta) v'_d) + X_s' (V^2 - V \cos(\theta) v'_d - V \sin(\theta) v'_q) \right) \quad (11)$$

where  $(\cdot)^*$  denotes complex conjugate of the complex quantity,  $\text{Re}(\cdot)$  and  $\text{Im}(\cdot)$  denote the real and imaginary parts of a complex number, respectively. Parameters for different load types have been experimentally determined and reported [12], [17], [26], [34], [38]–[40].

### D. Load Inventory Concept

Load behavior will be modeled by using an aggregation of ZIP, exponential recovery and induction motor models from above with appropriate parameters selected for each to represent the load's components. This is shown conceptually in Figure 2 with the total complex power consumed  $P_L + jQ_L$  the sum of the power consumed by all the individual load elements. The parameters of interest will be the contribution coefficients  $\mu_i$  for  $i = 1, 2, \dots, N_L$  where  $N_L$  is the number of unique types of loads assumed to be connected to the bus as well as the initial conditions needed for each dynamic model.

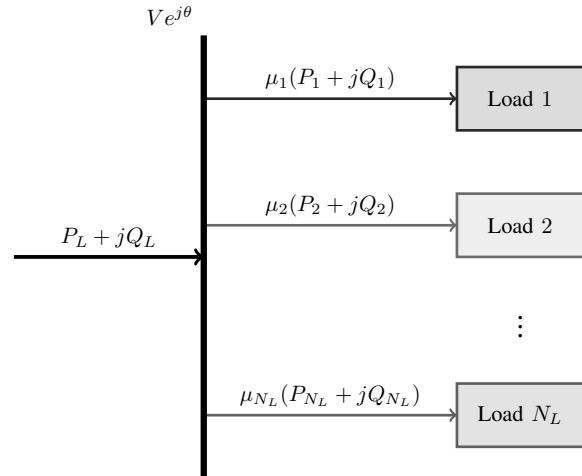


Fig. 2. Concept of load inventory

In summary, the aggregate load with average power  $P_L$  and reactive power  $Q_L$  will be the weighted sum of each individual type of model. Each model represents a candidate load that might exist in the inventory and its contribution (multiplier), indicated by  $\mu_i$ , is the parameter of interest for determining the inventory of loads. Total (aggregate)

complex power is the sum of all load powers

$$P_L + jQ_L = \mu_1(P_1 + jQ_1) + \mu_2(P_2 + jQ_2) + \dots + \mu_{N_L}(P_{N_L} + jQ_{N_L}). \quad (12)$$

### III. TRAJECTORY SENSITIVITIES

Differential-algebraic models are often utilized to represent the dynamic behavior of electric power systems [32]. When all loads are taken at a bus for the load inventory approach, the combined models presented above for loads can be represented in a manner similar to that of the broader power system:

$$\dot{x} = f(x, V) \quad (13)$$

$$y = g(x, V, \mu). \quad (14)$$

Here  $x$  is the vector of dynamic states (e.g.,  $x_p$ ,  $x_q$ ,  $v'_d$ ,  $v'_q$ ,  $s$  for dynamic loads) that satisfy the differential equations (13),  $y = [P_L, Q_L]^T$  is the  $2 \times 1$  vector of total average and reactive powers consumed by the aggregate load,  $V$  is the magnitude of the voltage at the bus (treated as an input) and  $\mu$  is the vector of contributions  $\mu_{i=1,2,\dots,N_L}$  taken as parameters.

Trajectory sensitivities provide a means to quantify the effect of small changes in parameters and/or initial conditions on a dynamic system's trajectory. Trajectory sensitivities will be utilized to guide the choice of how the parameters (here taken to be contributions  $\mu$  and initial conditions  $x_0$ ) should be altered to "best" match simulated trajectories to measurements of average power and reactive power consumed by the aggregate load. Following the presentation of trajectory sensitivities in [31], [32], flows of  $x$  and  $y$  that describe the response of (13), (14) are defined as

$$x(t) = \phi_x(\lambda, V, t) \quad (15)$$

$$y(t) = g(\phi_x(\lambda, V, t), \lambda, V, t) = \phi_y(\lambda, V, t) \quad (16)$$

where  $x(t)$  satisfies (13), all parameters of interest are combined into the vector  $\lambda = [x_0, \mu]^T$  of dimension  $M \times 1$ , and flows show the dependence of the trajectories on parameters  $\lambda$  (here initial conditions and fractional contributions), input  $V$  and time  $t$ . To obtain the sensitivity of the trajectories to small changes in the parameters  $\Delta\lambda$ , a Taylor series expansion of (15), (16) can be formed. Neglecting higher order terms in the expansion yields

$$\Delta x(t) = \phi_x(\lambda + \Delta\lambda, V, t) - \phi_x(\lambda, V, t) \quad (17)$$

$$\approx \frac{\partial \phi_x(\lambda, V, t)}{\partial \lambda} \Delta\lambda \equiv x_\lambda(t) \Delta\lambda \quad (18)$$

$$\Delta y(t) = \phi_y(\lambda + \Delta\lambda, V, t) - \phi_y(\lambda, V, t) \quad (19)$$

$$\approx \frac{\partial \phi_y(\lambda, V, t)}{\partial \lambda} \Delta\lambda \equiv y_\lambda(t) \Delta\lambda. \quad (20)$$

The time-varying partial derivatives  $x_\lambda$  and  $y_\lambda$  are known as the trajectory sensitivities, and can be obtained by differentiating (13) and (14) with respect to  $\lambda$ . This differentiation gives

$$\dot{x}_\lambda = f_x(t)x_\lambda \quad (21)$$

$$y_\lambda = g_x(t)x_\lambda + g_\lambda(t) \quad (22)$$

where  $f_x \equiv \frac{\partial f}{\partial x}$ ,  $g_x \equiv \frac{\partial g}{\partial x}$  and  $g_\lambda \equiv \frac{\partial g}{\partial \lambda}$  are time-varying Jacobian matrices, and  $f_\lambda \equiv \frac{\partial f}{\partial \lambda} = 0$ . Along the trajectory of the aggregate loads described by (13), (14) the trajectory

sensitivities will evolve according to the linear, time-varying differential equations (21), (22). Initial conditions for  $x_\lambda$  are obtained from (15) by noting  $x(t_0) = \phi_x(\lambda, V, t_0) = x_0$  such that  $x_\lambda(t_0) = [I, 0]$  which is a matrix with the same number of rows as states in  $x$  and number of columns equal to the number of parameters  $M$  [31], [41].  $I$  is the identity matrix and  $0$  is a matrix of zeros. Initial conditions for  $y_\lambda$  follow directly from the algebraic equation (22) to yield  $y_\lambda(t_0) = g_x(t_0) + g_\lambda(t_0)$ .

The  $N \times M$  sensitivity matrix for the  $i$ th output  $y^i$  is now defined by taking sensitivities (22) at discrete times  $t_{k=0,1,\dots,N-1}$

$$S^i(\lambda^j) = \begin{bmatrix} y_\lambda^i(t_0) \\ y_\lambda^i(t_1) \\ \vdots \\ y_\lambda^i(t_{N-1}) \end{bmatrix} \quad (23)$$

where  $N$  is the number of discrete values of time at which values are taken from the trajectory sensitivity (22) found by numerically solving the coupled system (13), (14), (21), (22);  $M$  is the number of parameters in  $\lambda$ ;  $\lambda^j$  is the particular set of values for parameters used when computing the trajectory and associated sensitivities; and for this particular application  $y_\lambda^1 = P_{L\lambda}$ ,  $y_\lambda^2 = Q_{L\lambda}$  and the complete sensitivity matrix  $S(\lambda^j) = \begin{bmatrix} S^1(\lambda^j) \\ S^2(\lambda^j) \end{bmatrix}$  is of dimension  $2N \times M$ .

As an example of computing the equations that will be solved for trajectory sensitivities, assume the total power is given by (12) and  $P_1$ ,  $Q_1$  are consumed by a load represented as the exponential recovery model's powers (3), (4). The sensitivities of  $P_L$ ,  $Q_L$  to parameter  $\mu_1$  are

$$\frac{\partial P_L}{\partial \mu_1} \equiv P_{L\mu_1} = P_1 = \frac{x_p}{T_p} + P_0 \left(\frac{V}{V_0}\right)^{\alpha t} \quad (24)$$

$$\frac{\partial Q_L}{\partial \mu_1} \equiv Q_{L\mu_1} = Q_1 = \frac{x_q}{T_q} + Q_0 \left(\frac{V}{V_0}\right)^{\beta t} \quad (25)$$

where the states  $x_p$ ,  $x_q$  will come from numerical solution of (5), (6) and  $V$  will be a specified input. The sensitivities of  $P_L$ ,  $Q_L$  to the initial conditions  $x_p(0)$ ,  $x_q(0)$  are

$$\frac{\partial P_L}{\partial x_p(0)} \equiv P_{Lx_p(0)} = \mu_1 \frac{1}{T_p} \frac{\partial x_p}{\partial x_p(0)} = \mu_1 \frac{1}{T_p} x_{p_{x_p(0)}} \quad (26)$$

$$\frac{\partial P_L}{\partial x_q(0)} \equiv P_{Lx_q(0)} = 0 \quad (27)$$

$$\frac{\partial Q_L}{\partial x_p(0)} \equiv Q_{Lx_p(0)} = 0 \quad (28)$$

$$\frac{\partial Q_L}{\partial x_q(0)} \equiv Q_{Lx_q(0)} = \mu_1 \frac{1}{T_q} \frac{\partial x_q}{\partial x_q(0)} = \mu_1 \frac{1}{T_q} x_{q_{x_q(0)}} \quad (29)$$

where the sensitivities  $x_{p_{x_p(0)}} \equiv \frac{\partial x_p}{\partial x_p(0)}$ ,  $x_{q_{x_q(0)}} \equiv \frac{\partial x_q}{\partial x_q(0)}$  will be the solution to the following differential equations that govern the trajectory sensitivities found by differentiating (5), (6) with respect to the initial conditions  $x_p(0)$ ,  $x_q(0)$

$$\frac{\partial}{\partial x_p(0)} \dot{x}_p \equiv \dot{x}_{p_{x_p(0)}} = -\frac{1}{T_p} \frac{\partial x_p}{\partial x_p(0)} = -\frac{1}{T_p} x_{p_{x_p(0)}} \quad (30)$$

$$\frac{\partial}{\partial x_q(0)} \dot{x}_p \equiv \dot{x}_{p_{x_q(0)}} = 0 \quad (31)$$

$$\frac{\partial}{\partial x_p(0)} \dot{x}_q \equiv \dot{x}_{q_{x_p(0)}} = 0 \quad (32)$$

$$\frac{\partial}{\partial x_{q(0)}} \dot{x}_q \equiv \dot{x}_{q_{xq(0)}} = -\frac{1}{T_q} \frac{\partial x_q}{\partial x_{q(0)}} = -\frac{1}{T_q} x_{q_{xq(0)}}. \quad (33)$$

Note the order of the derivatives (with respect to parameter and time) were interchanged in the process.

The differential equations (30), (33) that govern the trajectory sensitivities are solved numerically in parallel with the differential equations (5), (6) that govern the model such that trajectories are obtained for both. Calculations of sensitivities for all load models to all parameters are given in [27]. Ma et al. [17] also present trajectory sensitivities for an induction motor's internal parameters, and use them to determine which parameters have observable effects on measured quantities.

#### IV. PARAMETER ESTIMATION

Parameter estimation will be cast as a nonlinear least squares problem and solved using a Gauss-Newton iterative procedure [32]. Measurements of average and reactive power consumed by a load during a disturbance will be used to estimate the unknown model parameters (here contributions and initial conditions). The aim of parameter estimation is to determine parameter values that achieve the closest match between the measured samples and the model's simulated trajectory. Let measurements of the total average power  $P_L$  and reactive power  $Q_L$  (denoted by  $P_{L_m}$  and  $Q_{L_m}$ , respectively) consumed by the aggregate load be given by the appended sequences of  $N$  measurements

$$\vec{y}_m = \begin{bmatrix} [P_{L_m}(t_0), P_{L_m}(t_1), \dots, P_{L_m}(t_{N-1})]^T \\ [Q_{L_m}(t_0), Q_{L_m}(t_1), \dots, Q_{L_m}(t_{N-1})]^T \end{bmatrix} \quad (34)$$

with the corresponding simulated trajectory from numerically solving (13), (14) given by

$$\vec{y} = \begin{bmatrix} [P_L(t_0), P_L(t_1), \dots, P_L(t_{N-1})]^T \\ [Q_L(t_0), Q_L(t_1), \dots, Q_L(t_{N-1})]^T \end{bmatrix} \quad (35)$$

to get corresponding values at times  $t_{k=0,1,2,\dots,N-1}$ . The mismatch between the measurements and corresponding model's trajectory can be written in vector form as

$$\vec{e}(\lambda) = \vec{y}(\lambda) - \vec{y}_m \quad (36)$$

where the notation is used to show the dependence of the trajectory, and correspondingly the error, on the parameters  $\lambda$ . The vectors  $\vec{e}$ ,  $\vec{y}$  and  $\vec{y}_m$  will be of dimension  $2N \times 1$  as  $N$  measurements of  $P_L$  and  $Q_L$  are assumed. The best match between model and measurement is obtained by varying the parameters so as to minimize the error vector  $\vec{e}(\lambda)$  by some measure. One common measure is the two-norm (sum of squares) of the error vectors expressed as a cost function

$$C(\lambda) = \frac{1}{2} \|\vec{e}(\lambda)\|_2^2 = \frac{1}{2} \sum_{k=0}^{2N-1} e_k(\lambda)^2. \quad (37)$$

The error  $e_k(\lambda)$  is the  $k$ th element of  $\vec{e}$  and can be linearly approximated via a Taylor series expansion about an initial value of  $\lambda = \lambda^j$  which yields

$$e_k(\lambda) \approx e_k(\lambda^j) + \frac{\partial e_k(\lambda^j)}{\partial \lambda} (\lambda - \lambda^j) \quad (38)$$

$$= e_k(\lambda^j) + y_{\lambda k}(\lambda^j) \Delta \lambda \quad (39)$$

where  $\frac{\partial e_k(\lambda^j)}{\partial \lambda} = \frac{\partial y_k(\lambda^j)}{\partial \lambda} = y_{\lambda k}(\lambda^j)$  since the measurements  $y_{m_k}$  are independent of  $\lambda$  and the definition  $\Delta \lambda = \lambda - \lambda^j$  is

utilized. The new value of  $\lambda^j$  denoted  $\lambda^{j+1}$  will be chosen to minimize the following cost function with linearized error.

$$\begin{aligned} C(\lambda) &= \frac{1}{2} \sum_{k=0}^{2N-1} (e_k(\lambda^j) + y_{\lambda k}(\lambda^j) \Delta \lambda)^2 \\ &= \frac{1}{2} \sum_{k=0}^{2N-1} (e_k(\lambda^j) + S_k(\lambda^j) \Delta \lambda)^2 \\ &= \frac{1}{2} \|\vec{e}(\lambda^j) + S(\lambda^j) \Delta \lambda\|_2^2 \end{aligned} \quad (40)$$

where  $S_k$  is the  $k$ th row of the sensitivity matrix  $S$ .

Minimizing the cost function of linearized error (40) can now be performed via the Gauss-Newton method [32]. The process starts with an initial guess  $\lambda^0$  for parameter values and then parameters are updated according to iterations of the following two steps.

$$S(\lambda^j)^T S(\lambda^j) \Delta \lambda^{j+1} = -S(\lambda^j)^T e(\lambda^j) \quad (41)$$

$$\lambda^{j+1} = \lambda^j + \alpha^{j+1} \Delta \lambda^{j+1} \quad (42)$$

where  $S$  is the trajectory sensitivity matrix defined in (23),  $\alpha^{j+1}$  is a scalar that determines step size, and iterations stop when  $\Delta \lambda^{j+1}$  is sufficiently small. The resulting parameter values  $\lambda^{j+1}$  will be a local minimum for the cost function (37) due to the linearization and will be dependent on the initial guess  $\lambda^0$ . An additional note is that the parameter estimation process breaks down if  $S^T S$  is ill-conditioned, i.e., nearly singular. This leads to the concept of identifiability and quantification of parametric effects [17], [32], [42], [43]. The invertibility of  $S^T S$  can be investigated through its singular values and condition number, eigenvalues, or magnitude of sensitivities over a trajectory via the 2-norm. The less-rigorous, 2-norm will be utilized here to gain insight into the condition of  $S^T S$ . The 2-norm will be defined for the sensitivity of the  $i$ th output  $y^i$  to the  $j$ th parameter  $\lambda_j$  summed over discrete times  $t_k$  as

$$\|S^{ij}\|_2^2 = \sum_{k=0}^{N-1} S^{ij}(t_k, \lambda)^2. \quad (43)$$

The size of the values computed via (43) will give an indication of the effect of parameters on the trajectory, and in turn give guidance as to which parameters can be estimated.

#### V. APPLICATION TO ONE BUS VIA SIMULATION

The parameter estimation approach described above was implemented through simulation to estimate load contributions and initial conditions. Five loads, each represented by one of five models, were taken as connected to a bus as shown in Figure 2 with magnitude  $V$  of the bus's phasor voltage taken to be the input to the models, and average and reactive powers  $P_L$ ,  $Q_L$ , respectively, taken to be the (measurable) outputs. Load 1 was an exponential recovery model, load 2 was the model of a residential induction motor, load 3 was a model of a small industrial induction motor, load 4 was a model of a large industrial induction motor, and load 5 was a ZIP model. That made the  $M = 16$  unknown parameters

$$\lambda = [x_{p1}(0), x_{q1}(0), v'_{d2}(0), v'_{q2}(0), s_2(0), v'_{d3}(0), v'_{q3}(0), s_3(0), v'_{d4}(0), v'_{q4}(0), s_4(0), \mu_1, \mu_2, \mu_3, \mu_4, \mu_5]^T \quad (44)$$

which includes initial conditions for all the states in the individual models as well as the fractional contributions of

each load model to the aggregate power consumed. For the five loads considered, the total load is given by

$$\begin{aligned}
 P_L + jQ_L &= \mu_1(P_1 + jQ_1) + \mu_2(P_2 + jQ_2) \\
 &+ \mu_3(P_3 + jQ_3) + \mu_4(P_4 + jQ_4) \\
 &+ \mu_5(P_5 + jQ_5)
 \end{aligned} \quad (45)$$

with  $N_L = 5$ ;  $\mu_{i=1,2,\dots,5}$  the fractional contributions of each load model;  $P_1, Q_1$  given by (3), (4);  $P_2, Q_2$  given by (10), (11);  $P_3, Q_3$  given by (10), (11);  $P_4, Q_4$  given by (10), (11); and  $P_5, Q_5$  given by (1), (2). Representative values for parameters used in each model were taken from [8], [36], [38], [39] and are given in Table I, and the nominal bus voltage is taken to be  $V_0 = 1$ p.u.

TABLE I  
PARAMETER VALUES FOR MODELS OF LOADS

Load	Model and Parameters							
1	Exponential Recovery							
	$P_0$	$T_P$	$\alpha_s$	$\alpha_t$	$Q_0$	$T_q$	$\beta_s$	$\beta_t$
	1.25	60	0	2	0.5	60	0	2
2	Induction Motor - Residential							
	$R_s$	$X_s$	$X_m$	$R_r$	$X_r$	H	$T_0$	
	0.077	0.107	2.22	0.079	0.098	0.74	0.46	
3	Induction Motor - Small Industrial							
	$R_s$	$X_s$	$X_m$	$R_r$	$X_r$	H	$T_0$	
	0.031	0.1	3.2	0.018	0.18	0.7	0.6	
4	Induction Motor - Large Industrial							
	$R_s$	$X_s$	$X_m$	$R_r$	$X_r$	H	$T_0$	
	0.013	0.067	3.8	0.009	0.17	1.5	0.8	
5	ZIP							
	$P_0$	$K_{1p}$	$K_{2p}$	$K_{3p}$	$Q_0$	$K_{1q}$	$K_{2q}$	$K_{3q}$
	1.0	0.15	0.6	0.25	0.7	0.05	-0.05	1.0

### A. Results when no error in measurements

For study in simulation, a 3% decrease in the magnitude of the bus's voltage  $V$  was taken to be the input. The voltage was dropped from its nominal value of 1p.u. to 0.97p.u. at 50 seconds. With the initial conditions and load contributions at specified values, the simulation was run to generate synthetic, "measured" data to represent data that might be collected by a voltage disturbance monitor or phasor measurement unit. A sampling rate of 10Hz was used to record the total average and reactive powers consumed by the five loads. Nominal values for parameters are given in Table II, and plots of the aggregate power consumption  $P_L$  and  $Q_L$  are given in Figures 3 and 4, respectively, as the solid lines.

The simulation was then modified to run with initial guesses for parameter values, and the iterative Gauss-Newton process described by (41), (42) implemented to update the values of the parameters until they converged to within a specified tolerance. At each iteration, the system's model (13), (14) and trajectory sensitivities (21), (22) were numerically solved using Matlab's *ode15s()* solver for a new trajectory using updated values of the parameters. The results of the iterative process can be seen Figure 5 and show convergence of the load contributions to values used to create the synthetic measurements. The final, estimated values of all parameters (both initial conditions and load contributions) are given in Table II. The simulated trajectories for  $P_L$  and  $Q_L$

as the parameters are updated can be seen as the dashed lines in Figures 3 and 4.

TABLE II  
VALUES, GUESSES AND ESTIMATES OF PARAMETERS

Load	Model and Estimated Parameters				
1	Exponential Recovery				
		$x_p(0)$	$x_q(0)$	$\mu_1$	
	value:	0.0010	0.0007	0.1000	
	guess:	0.0025	0.0015	0.3000	
	estimate:	0.0010	0.0007	0.1000	
2	Induction Motor - Residential				
		$v'_d(0)$	$v'_q(0)$	$s(0)$	$\mu_2$
	value:	0.8659	0.1439	0.0399	0.2000
	guess:	0.9000	0.1800	0.0550	0.3000
	estimate:	0.8659	0.1439	0.0399	0.2001
3	Induction Motor - Small Industrial				
		$v'_d(0)$	$v'_q(0)$	$s(0)$	$\mu_3$
	value:	0.8842	0.0527	0.0120	0.2000
	guess:	0.9000	0.0750	0.0600	0.1000
	estimate:	0.8840	0.0527	0.0121	0.2001
4	Induction Motor - Large Industrial				
		$v'_d(0)$	$v'_q(0)$	$s(0)$	$\mu_4$
	value:	0.9124	0.0308	0.0078	0.3000
	guess:	0.8900	0.5000	0.0150	0.2000
	estimate:	0.9125	0.0308	0.0078	0.2999
5	ZIP				
				$\mu_5$	
	value:			0.2000	
	guess:			0.1000	
	estimate:			0.2000	

Convergence of Average Power to Simulated Measurements

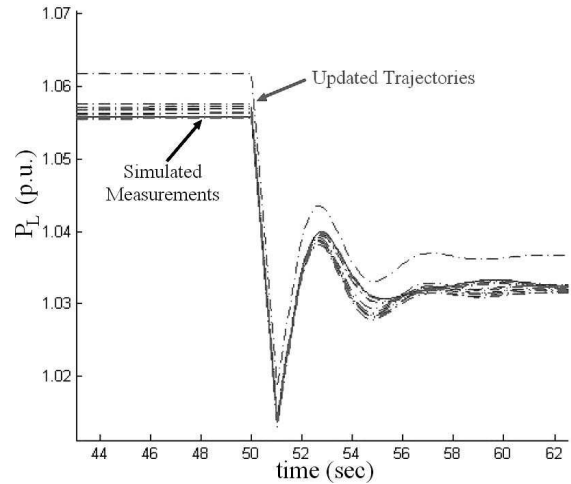


Fig. 3. Average power consumed by aggregate load; simulated measurements are solid line and trajectories for updated parameter estimates are dashed lines

### B. Study of identifiability

For the sample application above where no measurement error was introduced, the 2-norm of all sensitivities was calculated and shown in Table III. Of particular note is that the sensitivities of the average and reactive power are at least an order of magnitude larger for load contributions than initial conditions. This indicates that the load contributions have a larger impact on the trajectory and in turn should be

Convergence of Reactive Power to Simulated Measurements

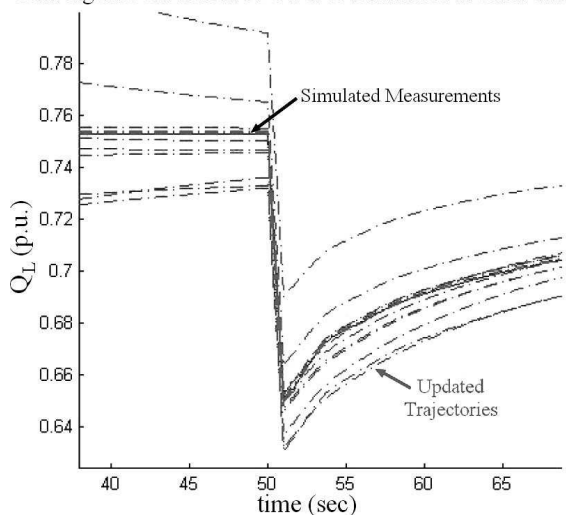


Fig. 4. Reactive power consumed by aggregate load; simulated measurements are solid line and trajectories for updated parameter estimates are dashed lines

Estimation of Load Composition Parameters

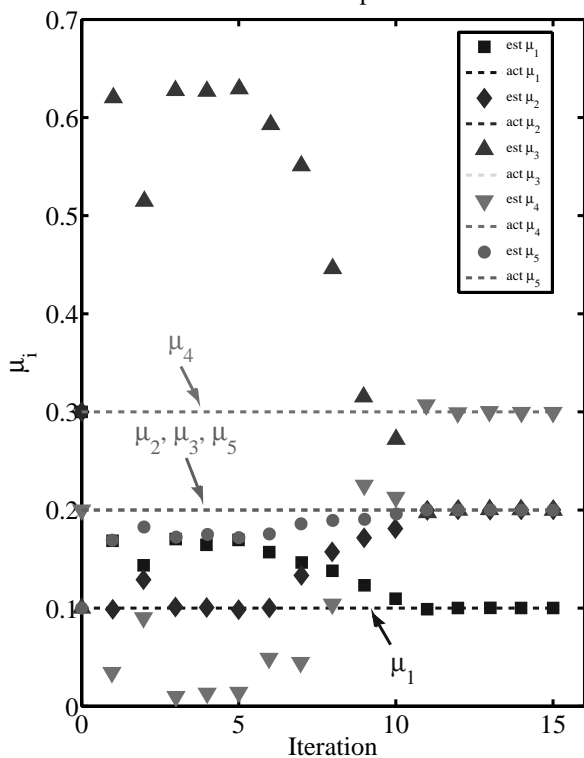


Fig. 5. Estimates of parameters (as markers/symbols) representing load contributions over iterations; dashed lines are actual values

more readily identified through parameter estimation. When no measurement error was assumed, both initial conditions and load contributions were identified, but when random error was introduced (as discussed in the next section) the estimates of the initial conditions were inaccurate. The zero entries in the table imply that the load models' powers do not depend on that particular parameter.

As an additional check of identifiability for the parameters of interest, both the condition number and eigenvalues were computed for the matrix  $S^T S$ . The condition number was  $2.281 \times 10^{15}$  with sensitivities for initial conditions included

TABLE III  
2-NORM OF TRAJECTORY SENSITIVITIES FOR PARAMETERS (LOAD CONTRIBUTIONS AND INITIAL CONDITIONS) OF INTEREST

Load	Model and 2-norm of Trajectory Sensitivities				
1	Exponential Recovery				
	$x_p(0)$	$x_q(0)$	$\mu_1$		
	$\ S_{P_L}\ _2^2$ :	0.029	0	7.920	
	$\ S_{Q_L}\ _2^2$ :	0	0.027	15.37	
2	Induction Motor - Residential				
	$v'_d(0)$	$v'_q(0)$	$s(0)$	$\mu_2$	
	$\ S_{P_L}\ _2^2$ :	0.005	0.003	0.002	14.37
	$\ S_{Q_L}\ _2^2$ :	0.002	0.001	0.001	13.59
3	Induction Motor - Small Industrial				
	$v'_d(0)$	$v'_q(0)$	$s(0)$	$\mu_3$	
	$\ S_{P_L}\ _2^2$ :	0.001	0.003	0.002	1.116
	$\ S_{Q_L}\ _2^2$ :	0.081	0.003	0.008	3.220
4	Induction Motor - Large Industrial				
	$v'_d(0)$	$v'_q(0)$	$s(0)$	$\mu_4$	
	$\ S_{P_L}\ _2^2$ :	0.004	0.003	0.003	4.095
	$\ S_{Q_L}\ _2^2$ :	0.009	0.005	0.007	4.725
5	ZIP				
				$\mu_5$	
	$\ S_{P_L}\ _2^2$ :			75.97	
	$\ S_{Q_L}\ _2^2$ :			64.89	

which confirmed an ill-conditioned matrix and potential difficulty in estimating initial conditions. When sensitivities were removed from  $S^T S$  leaving only those to load contributions, the condition number improved to 202.4 which indicated load contributions are identifiable. Eigenvalues of  $S^T S$  were computed and further confirmed identifiable parameters as small eigenvalues were associated with the initial conditions and much larger eigenvalues were associated with the load contributions.

### C. Results with 2% random error in measurements

The study described above was repeated, but this time with an error in each measurement achieved by adding a normally distributed random number to each measurement with mean 0 and standard deviation 2%. The method of estimating parameters worked well for the load contributions, but not the initial conditions. This is attributed to the issues with identifiability discussed above. Table IV shows the "true values", initial guesses and estimates of the parameters representing load contributions in this case.

## VI. APPLICATION TO 9-BUS SYSTEM VIA SIMULATION

The second application of the approach is through simulation of the Western System Coordinating Council (WSCC) three-machine, nine-bus test system shown in Figure 6 where details, parameters and a load flow solution are given in Sauer and Pai [44] and Dembart et al. [45]. The three generators are represented by two-axis machine models with IEEE-Type I excitors [44] and the transformers and transmission lines are modeled by admittances from which an admittance matrix, and ultimately power balance equations can be developed [33], [44]. The three loads at buses five, six and eight are taken to be combinations of various models presented in Section II.

The load at bus eight was taken to be the one of interest and consisted of two components connected to the bus

TABLE IV  
 VALUES, GUESSES AND ESTIMATES OF PARAMETERS WHEN 2%  
 RANDOM ERROR IN MEASUREMENTS

Load	Model and Estimated Parameters			
1	Exponential Recovery			
	$\mu_1$	value	guess	estimate
		0.1000	0.3000	0.1231
2	Induction Motor - Residential			
	$\mu_2$	value	guess	estimate
		0.2000	0.3000	0.1698
3	Induction Motor - Small Industrial			
	$\mu_3$	value	guess	estimate
		0.2000	0.1000	0.1740
4	Induction Motor - Large Industrial			
	$\mu_4$	value	guess	estimate
		0.3000	0.2000	0.3102
5	ZIP			
	$\mu_5$	value	guess	estimate
		0.2000	0.1000	0.2272

as shown conceptually in Figure 2. Component one was an exponential recovery model given by equations (3)-(6) and component two was the model of an induction motor given by equations (7)-(11). Representative parameters were selected to be consistent with those presented in [8], [12], [36], [38], [39] for both models and are provided in Table V. The unknown parameters are taken to be

$$\lambda = [\mu_1, \mu_2]^T \quad (46)$$

which are the  $M = 2$  contributions of each component's model to the aggregate average power  $P_L$  and reactive power  $Q_L$  via

$$P_L + jQ_L = \mu_1(P_1 + jQ_1) + \mu_2(P_2 + jQ_2) \quad (47)$$

where  $N_L = 2$ ;  $P_1, Q_1$  are given by (3), (4); and  $P_2, Q_2$  are given by (10), (11).

The scenario adopted to generate simulated measurements for bus eight's voltage  $V$ , and average and reactive powers  $P_L, Q_L$ , respectively, was to reduce bus five's load by 10%. This loss in load was enough to make the unknown parameters  $\lambda$  identifiable as discussed in Section V-B such that the approach to parameter estimation was viable. The simulated measurements of  $V, P_L$ , and  $Q_L$  at bus eight that result from the disturbance at bus five are shown in Figures 7, 8 and 9, respectively, where the sampling rate was 100 Hz and contributions of the load's components were taken to be  $\mu_1 = \mu_2 = 1.0$ .

 TABLE V  
 PARAMETER VALUES FOR MODELS OF LOADS AT BUS EIGHT

Load	Model and Parameters							
1	Exponential Recovery							
	$P_0$	$T_P$	$\alpha_s$	$\alpha_t$	$Q_0$	$T_q$	$\beta_s$	$\beta_t$
	0.497	150	0.5	1.75	0.1905	75	4	5
2	Induction Motor							
	$R_s$	$X_s$	$X_m$	$R_r$	$X_r$	H	$T_0$	
	0.046	0.097	2.571	0.056	0.115	0.627	1.073	

The simulation was then modified to run with initial guesses for parameter values now assumed to be unknown, and the iterative Gauss-Newton process described by (41),

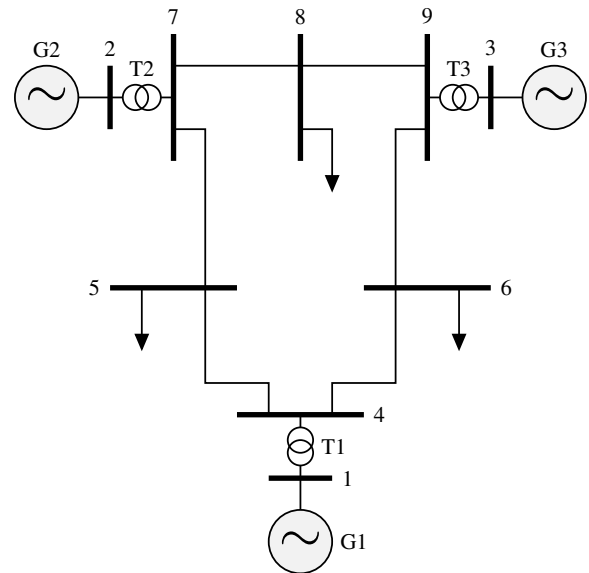


Fig. 6. One-line diagram of WSCC 9-bus system

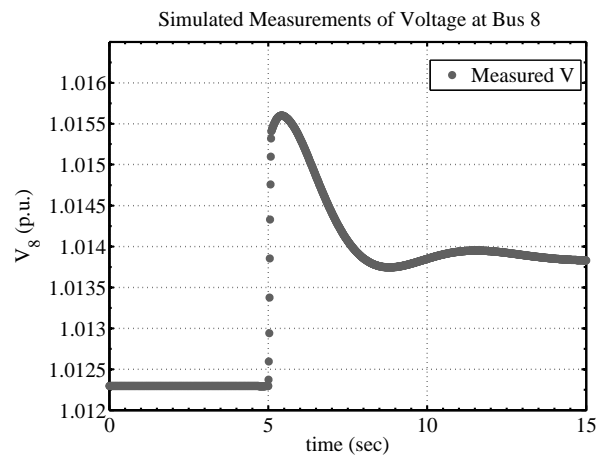


Fig. 7. Simulated measurements of magnitude of voltage at bus eight

(42) was implemented to update the values of the two parameters until they converged to within a specified tolerance. At each iteration, the system's model (13), (14) and trajectory sensitivities (21), (22) were numerically solved using Matlab's *ode15s()* solver for a new trajectory using updated values of the parameters. The results of the iterative process can be seen in Figure 10 and show convergence of the estimated contributions to actual values used to create the synthetic measurements. The simulated trajectories for  $P_L, Q_L$  are shown in Figures 11, 12, respectively, and show convergence of the simulated trajectories (lines in the figures) to the simulated measurements (large dots in figure) as the iterations proceed.

## VII. CONCLUSION

This paper presented an application of trajectory sensitivities and parameter estimation to estimate an aggregate load's composition. Two examples are presented using simulated data. The first example used five types of loads modeled by an exponential recovery model, three induction motor models with different parameters, and a ZIP model connected to a bus that experienced a step change in voltage. The

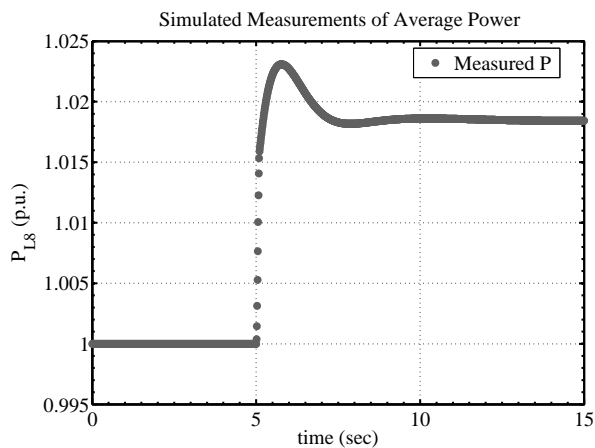


Fig. 8. Simulated measurements of average power consumed by aggregate load at bus eight

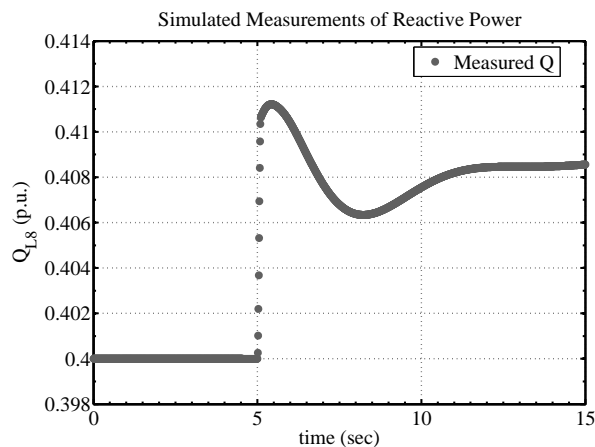


Fig. 9. Simulated measurements of reactive power consumed by aggregate load at bus eight

second example was the WSCC nine-bus system for which a disturbance enabled the contributions from two loads at a bus to be identified. Both simulation examples demonstrate that the approach has merit and holds promise for real-world application. Future work will be to incorporate and investigate additional models, and apply the approach to real data collected from a voltage disturbance monitor or phasor measurement unit.

## REFERENCES

- [1] A. Ellis, D. Kosterev, and A. Meklin, "Dynamic load models: Where are we?" in *Proceedings of the IEEE Power Engineering Society Transmission and Distribution Conference*, May 2006.
- [2] M. Gordon, "Impact of load behavior on transient stability and power transfer limitations," in *2009 IEEE Power and Energy Society General Meeting*, Calgary, AB, Canada, 2009.
- [3] IEEE Task Force on Load Representation for Dynamic Performance, "Bibliography on load models for power flow and dynamic performance simulation," *IEEE Transactions on Power Systems*, vol. 10, no. 1, pp. 523–538, Feb 1995.
- [4] IEEE Task Force on Load Representation for Dynamic Performance, "Load representation for dynamic performance analysis [of power systems]," *IEEE Transactions on Power Systems*, vol. 8, no. 2, pp. 472–482, May 1993.
- [5] D. Kosterev, A. Meklin, J. Undrill, B. Lesieutre, W. Price, D. Chassin, R. Bravo, and S. Yang, "Load modeling in power system studies: WECC progress update," in *Proceedings of the IEEE Power and Energy Society General Meeting - Conversion and Delivery of Electrical Energy in the 21st Century*, Jul 2008.

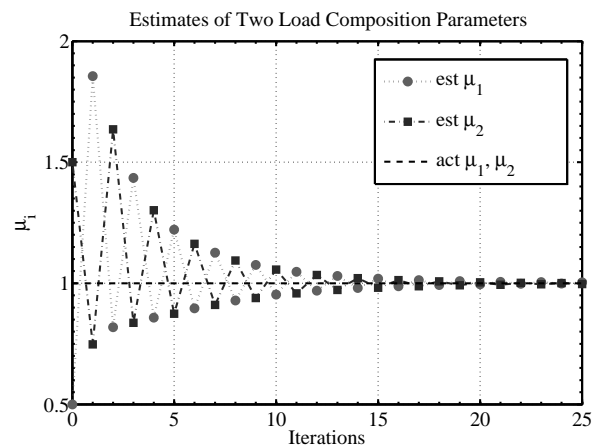


Fig. 10. Estimates of parameters (as markers/symbols) representing load contributions for bus eight over iterations; dashed line with fixed value of one represents actual values

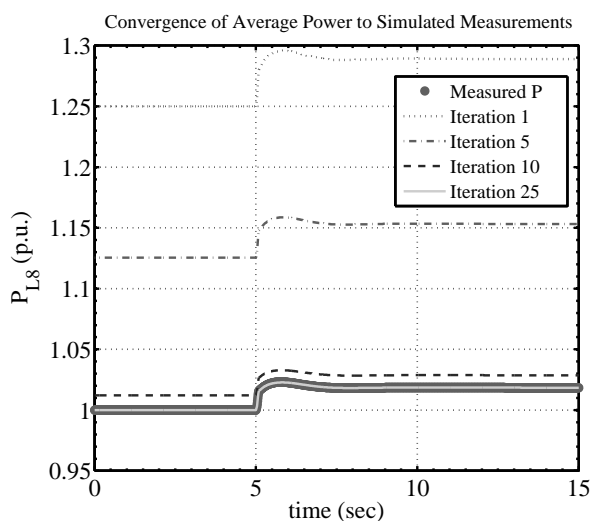


Fig. 11. Average power consumed by aggregate load; simulated measurements are large dots and trajectories (different line types) converge from top to bottom as estimates for parameters are updated

- [6] Y. Makarov, V. Maslennikov, and D. Hill, "Revealing loads having the biggest influence on power system small disturbance stability," *IEEE Transactions on Power Systems*, vol. 11, no. 4, pp. 2018–2023, Nov 1996.
- [7] Y. Mishra, Z. Dong, J. Ma, and D. Hill, "Induction motor load impact on power system eigenvalue sensitivity analysis," *IET Generation, Transmission and Distribution*, vol. 3, no. 7, pp. 690–700, 2009.
- [8] W. Price, K. Wirgau, A. Murdoch, J. V. Mitsche, E. Vaahedi, and M. El-Kady, "Load modeling for power flow and transient stability computer studies," *IEEE Transactions on Power Systems*, vol. 3, no. 1, pp. 180–187, Feb 1988.
- [9] J. V. Milanovic, K. Yamashita, S. Martinez Villanueva, S. Z. Djokic, and L. M. Korunovic, "International industry practice on power system load modeling," *IEEE Transactions on Power Systems*, vol. 28, no. 3, pp. 3038–3046, 2013.
- [10] S. A. Arefifar and W. Xu, "Online tracking of voltage-dependent load parameters using ULTC created disturbances," *IEEE Transactions on Power Systems*, vol. 28, no. 1, pp. 130–139, Feb 2013.
- [11] A. Bokhari, A. Alkan, R. Dogan, M. Diaz-Aguilo, F. de Leon, D. Czarkowski, Z. Zabar, L. Birenbaum, A. Noel, and R. Uosef, "Experimental determination of the ZIP coefficients for modern residential, commercial, and industrial loads," *IEEE Transactions on Power Delivery*, vol. 29, no. 3, pp. 1372–1381, Jun 2014.
- [12] C.-L. Chang and P.-H. Huang, "Load modeling study using measurement data for Taiwan power system," *Journal of Marine Science and Technology - Taiwan*, vol. 22, no. 5, pp. 643–649, Oct 2014.
- [13] B.-K. Choi, H.-D. Chiang, Y. Li, H. Li, Y.-T. Chen, D.-H. Huang, and M. G. Lauby, "Measurement-based dynamic load models: Derivation,



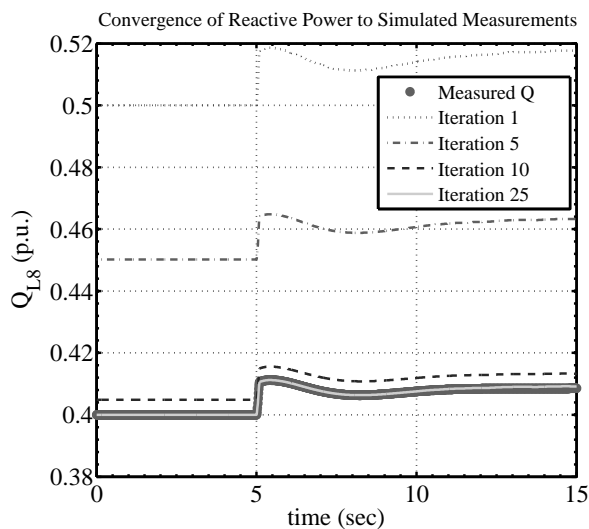


Fig. 12. Reactive power consumed by aggregate load; simulated measurements are large dots and trajectories (different line types) converge from top to bottom as estimates for parameters are updated

comparison, and validation," *IEEE Transactions on Power Systems*, vol. 21, no. 3, pp. 1276–1283, 2006.

- [14] D. Han, J. Ma, R.-m. He, and Z.-Y. Dong, "A real application of measurement-based load modeling in large-scale power grids and its validation," *IEEE Transactions on Power Systems*, vol. 24, no. 4, pp. 1756–1764, Nov 2009.
- [15] D. Karlsson and D. J. Hill, "Modelling and identification of nonlinear dynamic loads in power systems," *IEEE Transactions on Power Systems*, vol. 9, no. 1, pp. 157–166, Feb 1994.
- [16] Y. Li, H.-D. Chiang, B.-K. Choi, Y.-T. Chen, D.-H. Huang, and M. Lauby, "Representative static load models for transient stability analysis: Development and examination," *IET Generation, Transmission and Distribution*, vol. 1, no. 3, pp. 422–431, 2007.
- [17] J. Ma, D. Han, R.-M. He, Z.-Y. Dong, and D. J. Hill, "Reducing identified parameters of measurement-based composite load model," *IEEE Transactions on Power Systems*, vol. 23, no. 1, pp. 76–83, Feb 2008.
- [18] A. Maitra, A. Gaikwad, P. Zhang, M. Ingram, D. Mercado, and W. Woitt, "Using system disturbance measurement data to develop improved load models," in *Power Systems Conference and Exposition, 2006. PSCE '06. 2006 IEEE PES*, Oct 2006, pp. 1978–1985.
- [19] S. Ranade, A. Ellis, and J. Mechenbier, "The development of power system load models from measurements," in *2001 IEEE/PES Transmission and Distribution Conference and Exposition*, vol. 1, 2001, pp. 201–206.
- [20] H. Renmu, M. Jin, and D. Hill, "Composite load modeling via measurement approach," *IEEE Transactions on Power Systems*, vol. 21, no. 2, pp. 663–672, May 2006.
- [21] I. Visconti, L. De Souza, J. Costa, and N. Sobrinho, "Measurement-based load modelling of systems with dispersed generation," in *44th International Conference on Large High Voltage Electric Systems 2012*, Paris, France, 2012.
- [22] P. Zhang, "Measurement-based load modeling," Electric Power Research Institute (EPRI), Final Report 1014402, Sep 2006.
- [23] O. Abdalla, M. Bahgat, A. Serag, and M. El-Sharkawi, "Dynamic load modelling and aggregation in power system simulation studies," in *2008 12th International Middle East Power System Conference, MEPCON 2008*, Aswan, Egypt, 2008, pp. 270–276.
- [24] X. Liang, W. Xu, C. Y. Chung, W. Freitas, and K. Xiong, "Dynamic load models for industrial facilities," *IEEE Transactions on Power Systems*, vol. 27, no. 1, pp. 69–80, Feb 2012.
- [25] K. Morison, H. Hamadani, and L. Wang, "Practical issues in load modeling for voltage stability studies," in *IEEE Power Engineering Society General Meeting*, vol. 3, Jul 2003, pp. 1392–1397.
- [26] L. Pereira, D. Kosterev, P. Mackin, D. Davies, J. Undrill, and W. Zhu, "An interim dynamic induction motor model for stability studies in the WSCC," *IEEE Transactions on Power Systems*, vol. 17, no. 4, pp. 1108–1115, Nov 2002.
- [27] A. Patel, "Parameter estimation for load inventory models in electric power systems," MS thesis, New Mexico Institute of Mining and Technology, Socorro, NM, Dec 2008.
- [28] A. Patel, K. Wedeward, and M. Smith, "Parameter estimation for inventory of load models in electric power systems," in *Lecture Notes in Engineering and Computer Science: Proceedings of The World Congress on Engineering and Computer Science 2014, WCECS 2014*, San Francisco, USA, 22-24 October 2014, pp. 233–238.
- [29] D. R. Sagi, S. J. Ranade, and A. Ellis, "Evaluation of a load composition estimation method using synthetic data," in *Proceedings of the 37th Annual North American Power Symposium*, Oct 2005.
- [30] S. Ranade, D. Sagi, and A. Ellis, "Identifying load inventory from measurements," in *Proceedings of the IEEE Power and Energy Society Transmission and Distribution Conference and Exhibition*, May 2006.
- [31] I. A. Hiskens and M. A. Pai, "Power system applications of trajectory sensitivities," in *Proceedings of the Power Engineering Society Winter Meeting*, 2002.
- [32] I. A. Hiskens, "Nonlinear dynamic model evaluation from disturbance measurements," *IEEE Transactions on Power Systems*, vol. 16, no. 4, pp. 702–710, Nov 2001.
- [33] J. D. Glover, M. S. Sarma, and T. J. Overbye, *Power System Analysis and Design*, 4th ed. Thomson Learning, 2008.
- [34] P. Kundur, *Power system stability and control*, N. J. Balu and M. G. Lauby, Eds. McGraw-Hill, Inc., 1994.
- [35] D. J. Hill, "Nonlinear dynamic load models with recovery for voltage stability studies," *IEEE Transactions on Power Systems*, vol. 8, no. 1, pp. 166–176, Feb 1993.
- [36] I. R. Navarro, "Dynamic load models for power systems - estimation of time-varying parameters during normal operation," PhD thesis, Lund University, Lund, Sweden, Sep 2002.
- [37] A. Ellis, "Advanced load modeling in power systems," PhD thesis, New Mexico State University, Las Cruces, NM, Dec 2000.
- [38] IEEE Task Force on Load Representation for Dynamic Performance, "Standard load models for power flow and dynamic performance simulation," *IEEE Transactions on Power Systems*, vol. 10, no. 3, pp. 1302–1313, Aug 1995.
- [39] A. M. Najafabadi and A. T. Alouani, "Real time estimation of sensitive parameters of composite power system load model," in *Proceedings of the IEEE Power Engineering Society Transmission and Distribution Conference*, Orlando, FL, 2012.
- [40] F. Nozari, M. Kankam, and W. Price, "Aggregation of induction motors for transient stability load modeling," *IEEE Transactions on Power Systems*, vol. 2, no. 4, pp. 1096–1103, Nov 1987.
- [41] M. Hoffman, S. Schaffer, and K. Wedeward, "Parameter estimation in delayed-switching hybrid dynamical systems," in *IEEE Power Energy Society General Meeting, 2009. PES '09.*, Jul 2009.
- [42] I. A. Hiskens, "Identifiability of hybrid system models," in *Proceedings of the 2000 IEEE International Conference on Control Applications*, 2000.
- [43] J. Rose and I. A. Hiskens, "Estimating wind turbine parameters and quantifying their effects on dynamic behavior," in *Proceedings of the IEEE Power and Energy Society General Meeting - Conversion and Delivery of Electrical Energy in the 21st Century*, Jul 2008.
- [44] P. W. Sauer and M. A. Pai, *Power System Dynamics and Stability*. Upper Saddle River, NJ: Prentice Hall, 1998.
- [45] B. Dembart, A. Erisman, E. Cate, M. Epton, and H. Dommel, "Power system dynamic analysis: Phase I," Boeing Computer Services, Inc., Final Report EPRI-EL-484, Jul 1977.